Received July 8, 2021, accepted July 16, 2021, date of publication July 30, 2021, date of current version August 10, 2021.

Digital Object Identifier 10.1109/ACCESS.2021.3101321

A Four-Element Antenna Array System With 15 Reconfigurable Radiation Patterns

MARIOS PATRIOTIS[1], (Student Member, IEEE), FIRAS N. AYOUB[1], YOUSSEF TAWK[2], (Senior Member, IEEE), JOSEPH COSTANTINE[2], (Senior Member, IEEE), AND CHRISTOS G. CHRISTODOULOU[1], (Life Fellow, IEEE)

[1]Electrical and Computer Engineering Department, The University of New Mexico, Albuquerque, NM 87131, USA
[2]Electrical and Computer Engineering Department, American University of Beirut, Beirut 1107 2020, Lebanon

Corresponding author: Marios Patriotis (patriotism@unm.edu)

ABSTRACT This paper describes the design of a planar antenna array system with pattern reconfiguration in the azimuthal plane. The antenna array system is designed based on four antenna units where each unit is composed of two printed Yagi-Uda elements that radiate in directional beams over a dedicated sector, thus ensuring maximum isolation with neighboring units. The various units are fed on demand through a reconfigurable structure that is composed of four reconfigurable feeding networks and a one-to-four power divider. The feeding structure distributes the required power to the various radiating units through the activation of the two integrated PIN diodes along each of the four reconfigurable feeding networks. Such activation results in 15 reconfigurable radiation patterns that cover four orthogonal sectors over a fixed operating frequency, at 5.8 GHz. Each antenna unit is designed to exhibit a gain of 9 dBi with a half-power beamwidth of 44° and a sidelobe level of −16 dB. The antenna array is fabricated and tested, where the measured results validate the predicted simulated data.

INDEX TERMS Reconfigurable pattern, reconfigurable feeding network, sectoral antenna, pattern diversity.

I. INTRODUCTION

A reconfigurable antenna alters its operating behavior whether through frequency reconfiguration, radiation pattern agility, or polarization diversity in order to adapt to different deployment environments and applications [1]. More specifically, antennas with the ability to reconfigure their radiation patterns enable or block communication links on demand, cut out interferers and enhance the signal-to-noise ratio. This allows overcoming multiple communication channels adversities such as multipaths and fading [2]. Hence, antennas that exhibit a multitude of reconfigurable beams must be able to radiate on-demand and independently from each other.

The antenna operation is versatile and can meet the application needs of both, terrestrial and space communication systems. For terrestrial communication systems, this antenna can be implemented in applications that vary from the Internet of Things, where the multi-beam antenna can serve as a better candidate for spatial multiplexing or decreased packet collision [3], or cognitive radio for selective communication links accompanied with spatial filtering through directional beams [4]. On the other hand, this antenna can be implemented for space application in a cluster of small satellites to reduce interference through lobe deactivation of signal loss mitigation [5].

There are multiple techniques that can be employed to achieve active pattern reconfiguration. Several researchers have resorted to a plethora of interventions such as parasitic metal sections, feeding network reconfigurations, and switching between radiators [2]–[19]. The ability to achieve beam reconfiguration using parasitic metal strips is presented in [2], [5]–[7], where a center-driven element such as a dipole or a monopole is surrounded by metal strips that act as parasitic elements. The length of these metallic parasitic strips can be actively altered by relying on switches, varactor diodes, or through the implementation of liquid metal. Hence, the electromagnetic behavior of these elements enables the switching from a director to a reflector, which impacts the antenna's radiation pattern performance.

Reconfiguring the feeding network of an antenna system is another technique that results in pattern reconfiguration as discussed in [3], [4], [8]–[19]. Such reconfiguration method either relies on feeding specific antenna elements at discrete times or rerouting the excitation signal into different positions

The associate editor coordinating the review of this manuscript and approving it for publication was Giovanni Angiulli.

across the feeding network. The reconfiguration of the feeding network can be executed through the incorporation of single pole multiple throw switches along with delay [10]–[12]. This results in a beam steering capability that adds to the reconfigurable pattern of the antenna system. Other reconfiguration techniques employ radio frequency switches to connect and disconnect microstrip lines to active antenna elements as discussed in [13]–[16]. This technique enables agile antenna structure integration by relying on dynamic reconfiguration mechanisms through the rerouting and intentional alteration of the antenna surface currents. Another approach presented in [17], [18] enables multiple radiating elements to be instantaneously activated through the implementation of dynamic matching sections.

The work presented in this paper develops a novel reconfigurable feeding network that ensures the simultaneous activation of four radiating elements to result in 15 possible radiation patterns at the same operating frequency of 5.8 GHz. The needs for pattern reconfiguration arise from the importance of maintaining a single frequency band operation for a multitude of beam radiation directions. The antenna elements are designed as part of an end-fire planar Yagi-Uda antenna array in a cross-like configuration. Section II of this paper introduces the design of the four-element reconfigurable antenna array system along with a detailed analysis of the various parts of the feeding network. Section III presents the fabricated prototype and the corresponding measured results. Section IV concludes the paper.

II. PATTERN RECONFIGURABLE ANTENA ARRAY SYSTEM

An antenna array system that is composed of three main blocks is presented in this paper. The antenna array system, shown in Fig. 1, covers a total area of 133 mm × 133 mm. The first block (`Block 1a, 1b, 1c, 1d`) consists of four identical radiating units that are designed on top of a 0.79 mm thick Rogers RT5870 substrate with a dielectric constant $\varepsilon_r = 2.33$, and a loss tangent $\tan\delta = 0.0012$. The four radiating units are positioned at the four corners of a cross-like arrangement. The second block (`Block 2a, 2b, 2c 2d`) is composed of four identical reconfigurable feeding networks that feed the four radiating units on demand through the activation of the appropriate PIN diodes. More specifically, two PIN diodes are integrated along each block to enable the rerouting of the RF signal for radiation pattern reconfigurability. The third block (`Block 3`) is the one-to-four power divider that distributes the input signal into the different radiating units (`Block 1`) through the reconfigurable feeding network (`Block 2`).

A. BLOCK 1: TWO-ELEMENT RADIATING UNIT

Each radiating unit is composed of two dipole Yagi-Uda antenna elements as shown in Fig. 2(a). The antenna array is fed through an antipodal feeding configuration in order to reduce the overall size of the system. The length of the dipole is approximately $0.5\lambda_g$ at 5.8 GHz for matching purposes. The antenna array radiating structure is positioned at

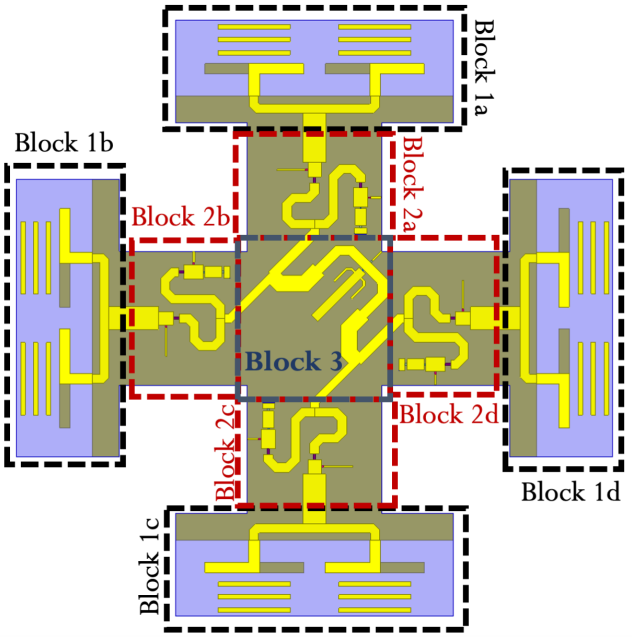

FIGURE 1. The proposed antenna system with 15 reconfigurable radiation patterns over four different sectors in the azimuthal plane.

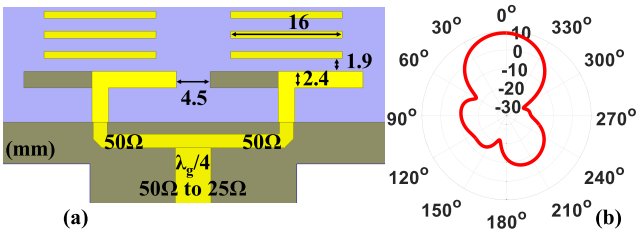

FIGURE 2. (a) The design of the radiating unit (Block 1), (b) The corresponding gain pattern at 5.8 GHz.

a distance of $0.15\lambda_g$ from the backside ground plane, which acts as a reflector. The directivity of each radiating unit is enhanced by incorporating in front of the dipole elements, three parasitic copper lines, each of length 16 mm and separated by 1.9 mm, to act as directors. The corresponding gain pattern of the array structure, shown in Fig. 2(b) with a maximum gain of 9 dBi, HPBW of 44°, and a sidelobe level of −16dB, enables the overall presented array structure to maintain high isolation between the independently activated beams of the four orthogonal sectors along the azimuthal plane.

B. BLOCK 2: RECONFIGURABLE FEEDING NETWORK

A reconfigurable feeding network is designed in order to enable the overall antenna array system to independently radiate 15 distinct radiation patterns. The proposed feeding network that feeds one of the four radiating units, is shown in Fig. 3(a). Accordingly, the presented network is composed of one input port (`Inp. Port`) and two output ports. One of these output ports (`a.p.`) is connected to the

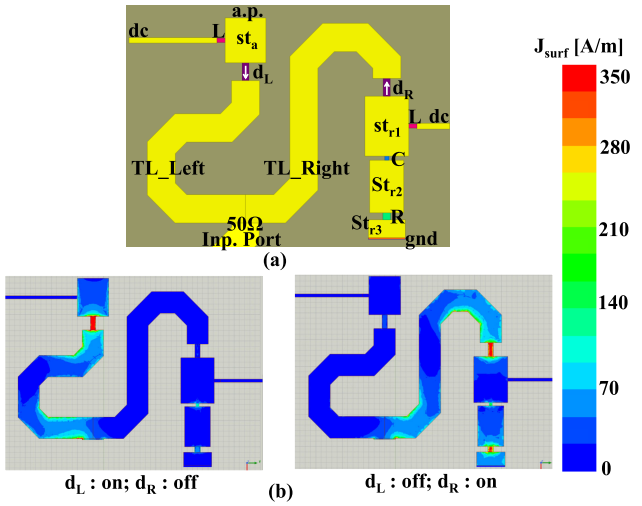

FIGURE 3. (a) The design of the reconfigurable feeding network (Block 2), (b) The change in the surface current for the two states of the integrated PIN diodes.

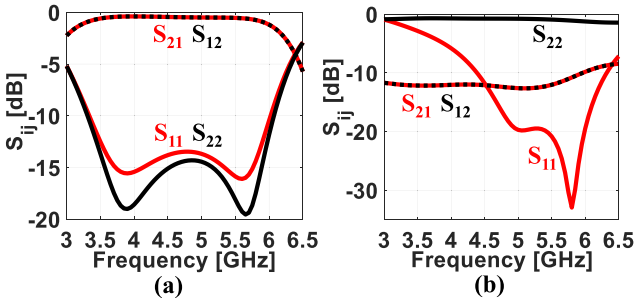

FIGURE 4. (a) The change in the S-parameters response of Block 2: (a) ON state, (b) OFF state.

corresponding radiating unit while the other port is terminated by R = 50 Ω load.

The feeding network consists of two 50 Ω parallel transmission lines (TL_Left and TL_Right) each of length 180°. These two TLs start from the input 50 Ω common port (Inp. Port) and are terminated by the two PIN diodes (d_L, d_R) from Skyworks (i.e., SMP1321-040LF, SC-79), [20]. The respective PIN diode with the 180° transmission line resembles a virtual open load at the input port when this PIN diode is in the OFF state. Consequently, the second PIN diode will be activated, and all the power is guided to the second TL. Thus, the operation mechanism of the proposed feeding network is based on activating each PIN diode individually. During the simulation process, the scattering parameters of the respective PIN diode are extracted from its datasheet and introduced into the simulation environment for more accurate performance estimation.

The surface currents, shown in Fig. 3(b), prove how the power is completely guided to one side of the feeding network based on the activation of the corresponding PIN diode. When dL: ON and dR: OFF, the supplied RF- current is routed to the fed radiating unit. However, when condition d_L: OFF and d_R: ON is applied, the RF current is guided and dissipated into the 50 Ω resistor load. This condition ensures no radiation from the corresponding array unit while maintaining good matching at the input port of the feeding network.

More specifically, TL_Left extends to the array unit's port (a.p.), through the diode d_L and the matching section st_a (3 mm × 3.2 mm). Whereas TL_Right extends to a load R = 50 Ω through the diode d_R, the matching section st_{r1} (3.2 mm × 4.3 mm), the DC-block capacitor C (9.9 pF), and the matching section St_{r2} (2.5 mm × 3.8 mm). The load resistor R is grounded through a TL section St_{r3} (2.5 mm × 1.3 mm). The DC bias of the two integrated PIN diodes is achieved through the RF-Choke inductors L (27 nH) and the two high RF-impedance lines (dc). The DC condition applied to activate each diode is 10 mA at 3V. The corresponding S-parameters of the feeding network for the two states (State 1 - d_L: ON, d_R: OFF) and (State 2 - d_L: OFF, d_R: ON) are presented in Fig. 4(a) and Fig. 4 (b). It is important to note that Port 1 corresponds to the input port (Inp. Port) of the feeding network while Port 2 corresponds to the array unit's port (a.p.). At the first state, the input and output reflection coefficients' bandwidths (S_{11}, $S_{22} < -10$ dB) are determined to be between 3.3 GHz and 6 GHz, with transmission coefficients ($S_{21|12}$ at 5.8 GHz) to reach −0.75 dB. On the other hand, when the second state is applied, S_{11} has a bandwidth that extends from 4.4 GHz up till 6.3 GHz and S_{22} is well mismatched, causing isolation greater than 10.8 dB.

C. BLOCK 3: POWER SPLITTER

The last block in the proposed antenna system design consists of a one-to-four power splitter that is designed in order to appropriately feed the four radiating units on demand through the activation of the corresponding feeding network. The layout of the designed power splitter is presented in Fig. 5(a) where the feeding input port is positioned at the center of the structure to acquire design uniformity and a reference point for the radiated beams of the overall array system.

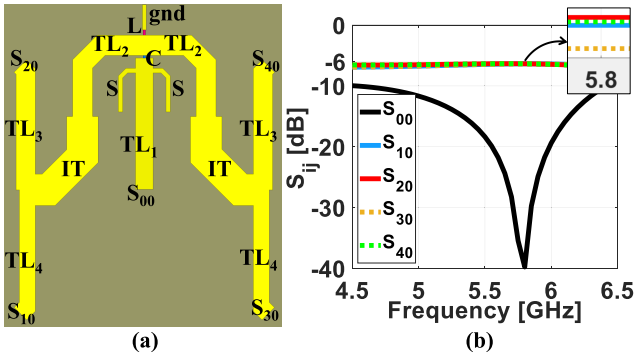

FIGURE 5. (a) The design of the one-to-four power divider (Block 3), (b) The corresponding S-parameters.

The power splitter is composed of the transmission line TL_1 (50 Ω, 155°) that extends to two identical transmission lines TL_2 (50 Ω, 142°) that are connected in parallel.

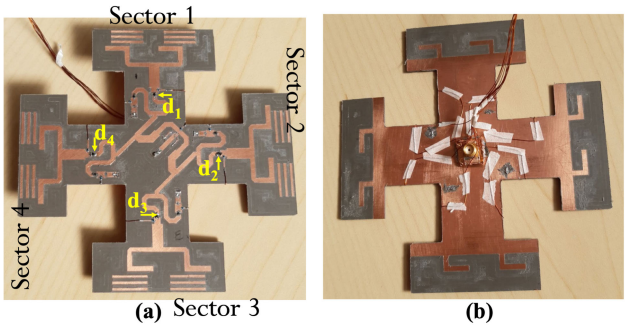

FIGURE 6. The fabricated prototype: (a) Top view with the four integrated PIN diodes, (b) bottom view with the DC wires.

This transition happens through a dc-block capacitor C (9.9 pF) for the RF source protection from any DC supplied to the various PIN diodes for activation. Two parallel stubs S (80 Ω, 25°) are integrated for proper matching at the design frequency of 5.8 GHz.

A quarter wavelength impedance transformer IT (35 Ω, 90°) is implemented to match each TL_2 to the two parallel connected transmission lines TL_3 (55 Ω, 148°) and TL_4 (63 Ω, 148°), respectively. The four transmission lines (TL_3 and TL_4) are used to feed the four reconfigurable feeding networks. It is important to note that the output impedance of these four lines is 50 Ω. However, the two designed TL_3 have slightly wider widths in order to account for the stronger coupling that these two TLs receive from the quarter wavelength impedance transformer IT section. The presented splitter also employs an RF-choke inductor L (27 nH) at its top center point to provide a common dc ground terminal to the integrated PIN diodes elements along with the four reconfigurable feeding networks.

The splitter's response presented in Fig. 5(b) shows an operation in the frequency range 4.5 GHz - 6.5 GHz. The transmission coefficient is almost the same for all the output ports and it reaches −6.38 dB at the design frequency of 5.8 GHz. Thus, providing the required one-to-four power split functionality.

III. PROTOTYPE MODEL AND MEASUREMENTS

The final step is the assembly of all the three designed blocks to form the prototype antenna system presented in Fig. 6. The four PIN diodes, highlighted in Fig. 6(a), provide a connection to the four radiating units. Four additional PIN diodes are also integrated to provide open load termination. The appropriate basing of these switches enables the overall antenna system to feature fifteen different states. These states can be described in a four binary digit number, where each digit describes the condition of each of the four sectors highlighted in Fig. 6(a). The sector with an active beam is identified with the number 1. On the other hand, a "blind" sector that does not radiate any beam, is identified with the number 0. As an example, condition 1000 can be interpreted as sector 1 is radiating while the rest do not. This is obtained by simultaneously activating the diode that connects to the radiating unit in the first sector and the PIN diodes that connect to the 50 Ω load in the other remaining three sectors. All remaining PIN diodes are deactivated.

To acquire the measurement data, the diodes are manually activated by connecting the dc wires on a stripboard. Nevertheless, in actual applications, the wires can be driven by a microcontroller that has a board with 9 dc sockets. The board can be assembled at the bottom side of the substrate, underneath the ground plane, in order not to interfere with the feeding network circuit that is on the top side. It is important to note that the proposed feeding network is coplanar with the radiating elements but does not disturb the radiation performance due to its well-matching at all of its ports. Therefore, it serves solely to route the power to the various components of the antenna structure.

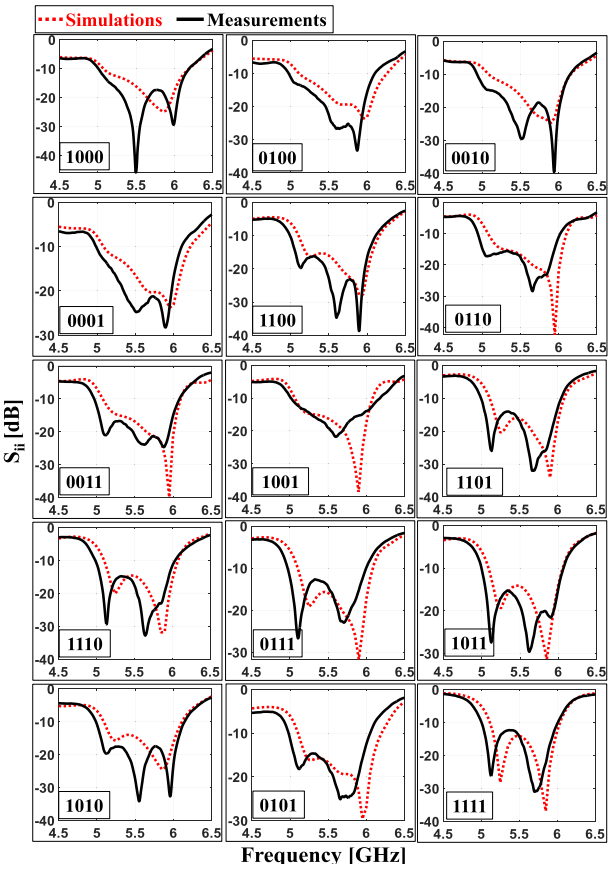

FIGURE 7. The simulated and measured input reflection coefficient of the overall antenna system for various states.

The measured input reflection coefficients of the fifteen states, compared to the simulated ones, are shown in Fig. 7. The overall antenna system provides an operational range of frequencies between 5 GHz and 6 GHz, with the antenna's main operating frequency at 5.8 GHz. For all the different biasing conditions, the proposed antenna system maintains a good impedance match and a close agreement between the simulated and measured data. The measured bandwidth

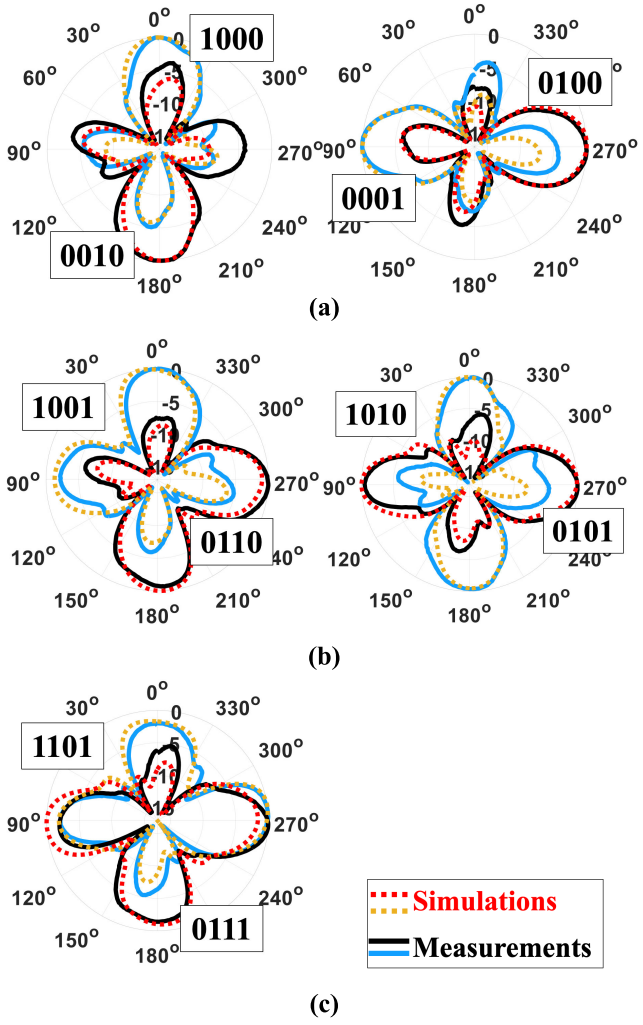

FIGURE 8. The simulated and measured reconfigurable radiation pattern for different cases: (a) One sector is active, (b) Two sectors are considered, and (c) Three active sectors.

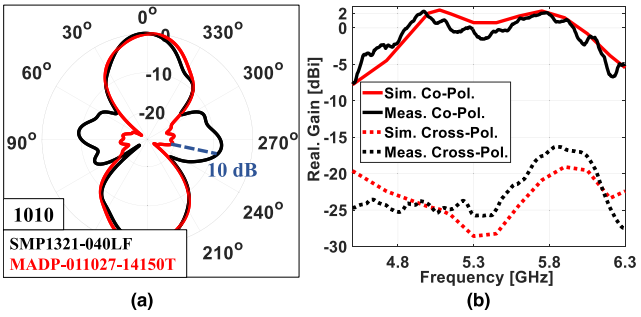

FIGURE 9. (a) The impact of low [20] and high [21] isolation RF switch on the radiation pattern. (b) The co/cross simulated and measured realized gain.

exhibits a slightly larger yet very conforming bandwidth. Such a small and acceptable difference is due to fabrication tolerances and various parasitic components.

The radiation patterns of the proposed antenna system are presented in Fig. 8(a) when activating only one sector. For this scenario, the presented antenna system is able to cover a dedicated sector along the azimuthal plane. The simulated and measured radiation patterns that correspond to some of the cases when two sectors are simultaneously activated are presented in Fig. 8(b). The activation of three sectors is summarized in Fig. 8(c). In total, the proposed antenna system is able to produce 15 different reconfigurable radiation patterns that are obtained to cover the four sectors on demand. A similar response is obtained for the remaining PIN diode states that are not included in Fig. 8. Accordingly, it is found that for all the 15 different radiation patterns, a good isolation between the active lobes of the corresponding sectors is obtained. This ensures minimum interference, less noise, and optimized performance. It is important to note that for all the scenarios, a great agreement is noticed between the simulated and measured radiation patterns as depicted in the various plots in Fig. 8. It is essential to emphasize that the PIN diode used in this work can be replaced with one that exhibits greater isolation at the off state, as the one in [21], and accordingly resulting in further diminished deactivated lobes. The corresponding gain patterns are shown in Fig. 9(a) where a drop of 10 dB is obtained in the deactivated lobe. Such gain pattern is plotted for the case when only two sectors are activated.

Fig. 9(b) shows the realized gain with respect to frequency for the co- and cross-polarization. At the desired frequency of 5.8 GHz, the gain is 1.9 dBi which results from the 9 dBi of the two-element planar array, the −6.38 dB transmission coefficient of the one-to-four power divider, and the roughly −0.75 dB transmission coefficient of the network in Fig. 3. The cross-polarization discrimination of the antenna is greater than 18.5 dB. The efficiency of the antenna system is also shown in Table 1 for the different switch configurations.

TABLE 1. Antenna efficiency [%].

Number of Active Elements	Simulated	Measured
4	86	82
3	65	62
2	47	44.9
1	30	28.6

The reconfigurable pattern capability of the proposed design is compared with respect to the latest works in the literature as presented in Table 2. This table shows that there is a great struggle to achieve a single driven port antenna with independent beam activation. As seen, most proposed designs implement SPMT (single pole multiple throw) switches that limit the antenna performance. The Figure of Merit (FoM) created in Eq. 1 helps to distinguish the new independent pattern capability of the proposed antenna. The FoM takes into account the number of the established reconfigurable

TABLE 2. Pattern reconfigurable antennas comparison.

Ref.	RF Ports	Elements	# Rec. Patterns	Indep. Beams	Method	FoM
[4]	1	6	12	2	RFN	4
[6]	1	4	4	1	PE	1
[9]	1	1	4	1	RGS	4
[10]	1	8	8	1	SPDT, SP4T	1
[11]	1	4	4	1	SP4T	1
[12]	1	4	4	1	SP4T	1
[14]	1	4	4	1	SP4T	1
[15]	1	4	4	1	RFN	1
[17]	1	4	11	3	RFN	8.25
This Work	**1**	**4**	**15**	**4**	**RFN**	**15**

RFN: Reconfigurable Feeding Network PE: Parasitic Elements
RGS: Reconfigurable Ground Slots

patterns and the beams that are independently activated with respect to the number of input RF ports and the radiating elements utilized.

$$\text{FoM} = \frac{(\#\text{ Rec. Patterns} * \#\text{ Indepen. Activ. Beams})}{(\#\text{ RF Ports} * \#\text{ Elements})} \quad \text{Eq. 1}$$

IV. CONCLUSION

This paper presents the design of a four-element reconfigurable antenna array that is capable of generating 15 radiation patterns. The reconfiguration potential of the full antenna system is driven by a reconfigurable feeding structure that employs active switching technique, reconfigurable power division, and high isolation factors to feed the different radiating units of the antenna system. Four radiating units compose the antenna system that are well isolated by relying on a plethora of techniques. Finally, once fed each unit radiates on demand a highly directive beam that can be sequentially reconfigured and rotated to cater for many applications. The antenna system is fabricated and measured, where measured results agree well with simulated data in terms of input matching as well as radiation pattern reconfigurability for the various activated sectors.

REFERENCES

[1] J. Costantine, Y. Tawk, S. E. Barbin, and C. G. Christodoulou, "Reconfigurable antennas: Design and applications," *Proc. IEEE*, vol. 103, no. 3, pp. 424–437, Mar. 2015.
[2] F. Farzami, S. Khaledian, B. Smida, and D. Erricolo, "Pattern-reconfigurable printed dipole antenna using loaded parasitic elements," *IEEE Antennas Wireless Propag. Lett.*, vol. 16, pp. 1151–1154, 2017.
[3] M.-I. Lai, T.-Y. Wu, J.-C. Hsieh, C.-H. Wang, and S.-K. Jeng, "Compact switched-beam antenna employing a four-element slot antenna array for digital home applications," *IEEE Trans. Antennas Propag.*, vol. 56, no. 9, pp. 2929–2936, Sep. 2008, doi: 10.1109/TAP.2008.928775.
[4] P.-Y. Wang, T. Jin, F.-Y. Meng, Y.-L. Lyu, D. Erni, Q. Wu, and L. Zhu, "Beam switching antenna based on a reconfigurable cascaded feeding network," *IEEE Trans. Antennas Propag.*, vol. 66, no. 2, pp. 627–635, Feb. 2018.
[5] X. Cai, A.-G. Wang, N. Ma, and W. Leng, "A novel planar parasitic array antenna with reconfigurable azimuth pattern," *IEEE Antennas Wireless Propag. Lett.*, vol. 11, pp. 1186–1189, 2012.
[6] Y.-F. Cheng, X. Ding, B.-Z. Wang, and W. Shao, "An azimuth-pattern-reconfigurable antenna with enhanced gain and front-to-back ratio," *IEEE Antennas Wireless Propag. Lett.*, vol. 16, pp. 2303–2306, 2017.
[7] M. S. Alam and A. M. Abbosh, "Wideband pattern-reconfigurable antenna using pair of radial radiators on truncated ground with switchable director and reflector," *IEEE Antennas Wireless Propag. Lett.*, vol. 16, pp. 24–28, 2017, doi: 10.1109/LAWP.2016.2552492.
[8] Y. Dong and T. Itoh, "Planar ultra-wideband antennas in Ku- and K-band for pattern or polarization diversity applications," *IEEE Trans. Antennas Propag.*, vol. 60, no. 6, pp. 2886–2895, Jun. 2012, doi: 10.1109/TAP.2012.2194680.
[9] J. Ouyang, Y. M. Pan, and S. Y. Zheng, "Center-fed unilateral and pattern reconfigurable planar antennas with slotted ground plane," *IEEE Trans. Antennas Propag.*, vol. 66, no. 10, pp. 5139–5149, Oct. 2018, doi: 10.1109/TAP.2018.2860046.
[10] M. Jeong, J. Kim, S. Bae, and W. Lee, "Miniaturised multi-beam-controlled circular eight-port beamforming network for long-range UHF RFID hemispheric coverage," *IET Microw., Antennas Propag.*, vol. 12, no. 2, pp. 154–159, Feb. 2018.
[11] P. Baniya and K. L. Melde, "Switched-beam endfire planar array with integrated 2-D Butler matrix for 60 GHz chip-to-chip space-surface wave communications," *IEEE Antennas Wireless Propag. Lett.*, vol. 18, no. 2, pp. 236–240, Feb. 2019, doi: 10.1109/LAWP.2018.2887259.
[12] H. Nakano, T. Abe, and J. Yamauchi, "Planar reconfigurable antennas using circularly polarized metalines," *IEEE Antennas Wireless Propag. Lett.*, vol. 18, no. 5, pp. 1006–1010, May 2019, doi: 10.1109/LAWP.2019.2907533.
[13] W. Lin, H. Wong, and R. W. Ziolkowski, "Wideband pattern-reconfigurable antenna with switchable broadside and conical beams," *IEEE Antennas Wireless Propag. Lett.*, vol. 16, pp. 2638–2641, 2017, doi: 10.1109/LAWP.2017.2738101.
[14] G. Jin, M. Li, L. Dan, and G. Zeng, "A simple planar pattern-reconfigurable antenna based on arc dipoles," *IEEE Antennas Wireless Propag. Lett.*, vol. 17, no. 9, pp. 1664–1668, Sep. 2018.
[15] Y. Tawk, J. Costantine, and C. G. Christodoulou, "An eight-element reconfigurable diversity dipole system," *IEEE Trans. Antennas Propag.*, vol. 66, no. 2, pp. 572–581, Feb. 2018.
[16] M. Patriotis, F. N. Ayoub, and C. G. Christodoulou, "Four-element beam switching antenna for compact IoT devices," in *Proc. 14th Eur. Conf. Antennas Propag. (EuCAP)*, Copenhagen, Denmark, Mar. 2020, pp. 1–4.
[17] J.-S. Row and C.-W. Tsai, "Pattern reconfigurable antenna array with circular polarization," *IEEE Trans. Antennas Propag.*, vol. 64, no. 4, pp. 1525–1530, Apr. 2016.
[18] P. Sanchez-Olivares, P. Sanchez-Dancausa, J. L. Masa-Campos, M. Iglesias-Menendez-de-la-Vega, and E. Garcia-Marin, "Circular conformal array antenna with omnidirectional and beamsteering capabilities for 5G communications in the 3.5-GHz range [Wireless Corner]," *IEEE Antennas Propag. Mag.*, vol. 61, no. 4, pp. 97–108, Aug. 2019.
[19] S. Tebache, A. Belouchrani, F. Ghanem, and A. Mansoul, "Novel reliable and practical decoupling mechanism for strongly coupled antenna arrays," *IEEE Trans. Antennas Propag.*, vol. 67, no. 9, pp. 5892–5899, Sep. 2019.
[20] *SMP1321 Series: Low Capacitance, Plastic Packaged PIN Diode*. Accessed: May 2021. [Online]. Available: https://www.skyworksinc.com/-/media/SkyWorks/Documents/Products/101-200/SMP1321_Series_200048Z.pdf
[21] *High Power PIN Diode 50 MHz–12 GHz*. Accessed: May 2021. [Online]. Available: https://cdn.macom.com/datasheets/MADP-011027-14150T.pdf

MARIOS PATRIOTIS (Student Member, IEEE) received the Diploma degree in electrical and computer engineering from the Democritus University of Thrace, Xanthi, Greece, in 2016, and the M.S. degree from The University of New Mexico, Albuquerque, NM, USA, in 2019, where he is currently pursuing the Ph.D. degree with the Antennas and RF Laboratory. His research interests include reconfigurable microwave matching networks and diversity antennas for millimeter-wave systems.

FIRAS N. AYOUB received the B.E. degree from the American University of Beirut, Beirut, Lebanon, in 2011, and the M.S. and Ph.D. degrees from The University of New Mexico, Albuquerque, NM, USA, in 2013 and 2018, respectively. He is currently an Assistant Research Professor with the ECE Department, The University of New Mexico, and a RF Engineer with TransCore. He is the co-inventor on two U.S. patents, and he has authored or coauthored more than 30 IEEE journal articles and conference papers. His research interests include mm-wave antennas, reconfigurable antenna arrays using nematic liquid crystal and reconfigurable RF components, and RFID.

YOUSSEF TAWK (Senior Member, IEEE) received the Bachelor of Engineering degree (Hons.) from Notre Dame University Louaize, in Fall 2006, the master's degree in engineering from the American University of Beirut, in 2007, and the Ph.D. degree from The University of New Mexico, Albuquerque, NM, USA, in 2011. He worked as the Valedictorian of his graduating class with Notre Dame University Louaize. He is currently an Assistant Professor with the ECE Department, American University of Beirut, Lebanon. He has more than 150 IEEE journal articles and conference papers many of which received finalist positions and honorable mentions in several paper contests. He is the coauthor of two books and one book chapter, and co-inventor on seven U.S. patents. His research interests include reconfigurable RF systems for microwave and mm-wave applications, cognitive radio, optically controlled RF components, phased arrays, and phase shifters based on smart RF materials. Throughout his education and career, he has received many awards and honors, such as the 2018 and 2014 Science and Technology Innovation Award for his patents on reconfigurable microwave filters and optically controlled antenna systems in addition to the 2011 IEEE Albuquerque Chapter Outstanding Graduate Award.

JOSEPH COSTANTINE (Senior Member, IEEE) received the bachelor's degree from the Second Branch of the Faculty of Engineering, Lebanese University, the master's (M.E.) degree from the American University of Beirut, and the Ph.D. degree from The University of New Mexico, in 2009. He is currently an Associate Professor with the Electrical and Computer Engineering Department, American University of Beirut, and a World Economic Forum Young Scientist. He has 11 provisional and full U.S. patents. He has published so far two books, one book chapter and more than 150 journal articles and conference papers. His research interests include reconfigurable antennas, cognitive radio, RF energy harvesting systems, antennas and rectennas for the IoT devices, RF systems for biomedical devices, wireless characterization of dielectric material, and deployable antennas for small satellites. He received many awards and honors throughout his career, including the 2008 IEEE Albuquerque Chapter Outstanding Graduate Award, the three year (2011–2013) Air Force Summer Faculty Fellowship with Kirtland's Space Vehicles Directorate in NM, USA, the 2017 First Prize at the Ideathon of International Healthcare Industry Forum, the 2019 Excellence in Teaching Award from the American University of Beirut, the 2018 and 2020 STC Science and Technology Innovation Awards, and the 2020 Distinguished Young Alumni Award from the School of Engineering at The University of New Mexico. Since July 2018, he has been an Associate Editor of the IEEE ANTENNAS AND WIRELESS PROPAGATION LETTERS.

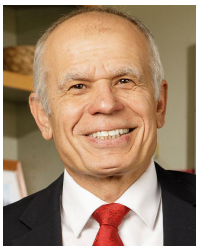

CHRISTOS G. CHRISTODOULOU (Life Fellow, IEEE) received the Ph.D. degree in electrical engineering from North Carolina State University, in 1985.

He is currently the Dean of the School of Engineering and Computing, The University of New Mexico (UNM). He is a Distinguished Professor with UNM. He has published over 570 articles in journals and conferences, written 17 book chapters, and coauthored nine books. He has several patents.

Dr. Christodoulou is a member of the Commission B of the U.S. National Committee (USNC) for URSI. He was a recipient of the 2010 IEEE John Krauss Antenna Award for his work on reconfigurable fractal antennas using MEMS switches and has been inducted in the Alumni Hall of Fame for the Electrical and Computer Engineering Department, North Carolina State University, in 2016. He served as an Associate Editor for the IEEE TRANSACTIONS ON ANTENNAS AND PROPAGATION for a period of six years. He served as a co-editor for a special issue on "Reconfigurable Systems" in the IEEE PROCEEDINGS, in March 2015, a co-editor of the IEEE Antennas and Propagation Special Issue on "Synthesis and Optimization Techniques in Electromagnetics and Antenna System Design," in March 2007, and for the Special Issue on "Antenna Systems and Propagation for Cognitive Radio," in 2014. Since 2013, he has been serving as a Series Editor for Artech House Publishing Company for the area of antennas and propagation. He was appointed as an IEEE AP-S Distinguished Lecturer (2007–2010).